

# Inertia: a New Force Field for Geometric Active Contour

Cui Hua and Wu Jianhua and Gao Liqun and Kong Zhi

**Abstract**—A new force field for geometric active contour, called inertia, is proposed in this paper. Based on analyzing the evolution process of geometric active contour and constructing extension velocities in level set method, it is found that geometric active contour can inherit its evolution velocities at the previous time step and has a tendency to keep its original movement state through integrating inertia force field into it. As an useful complementarity to the force field family for geometric active contour, inertia force can be integrated with other force fields to compose the coupling force field. Experimental results with several test images reveal that, compared with geodesic active contour integrated with gradient vector flow, geodesic active contour integrated with inertia and gradient vector flow, can enter into long, thin indentation of the objects' edge.

## I. INTRODUCTION

Active contours [1] are curves defined within an image domain that can move under the influence of the internal forces within the curve itself and external forces computed from the image data. They have been widely studied and their applications mainly include boundary extraction, shape modelling, segmentation of objects and motion tracking. There are two general types of active contour models: parametric active contours [1] (or snakes) and geometric active contour [2][3] (or geodesic active contour [3]).

The internal and external forces need be defined so that active contours will conform to an object boundary or other desired features within an image. The traditional force field has small capture range and is sensitive to the initial curve. In order that the curves converge the edges of objects well and truly, many improved force fields were put forwarded. Cohen [5] presented the balloon force, which enlarges the capture range of active contour, but can not enter into the concavities of the objects' edge. Xu and Prince [6] proposed gradient vector flow external force field, known as GVF, which solves the problem of small capture range and can go into the concavities of the objects' edge in principle. Chan and Vese proposed C-V method in [7]. It depends on the image information derived from homogenous regions and therefore it can obtain favorable results in fuzzy or discrete cases. However, in spite of these advantages, C-V method has an unavoidable restriction. That is, there are only two classes, the objects and the background. Paragios [9] integrated GVF into the geodesic active contour and proposed new

geometric flows for boundary extraction, which improved the segmentation effects of geodesic active contour.

Though gradient vector flow and other force fields were proposed to enlarge the capture range of external force field, it still seems difficult for contour curves to enter into long, thin intention of the objects' edge. In this paper we proposed inertia for geodesic active contour to address this problem. Inertia is constructed on the base of GVF force field. In the inertia force field, the evolving curves implicitly inherit their velocities at the previous time step and have the tendency to keep their original movement state.

This paper is organized as follows: In section 2, geodesic active contour and geometric flow integrated with GVF for boundary extraction are analyzed. In section 3, the proposed inertia force field and geometric flows integrated with inertia force for boundary extraction are explained and their numerical implementation is given. Section 4 describes the experimental results and gives an analytical discussion. Some concluding remarks are made in section 5.

## II. BACKGROUND

### A. Front Evolution and Level Set Theory

Let  $C(p,t)$ , defined as  $\{x(p,t),y(p,t)\}$  in 2D, denote a family of closed contours (i.e. curves) generated by evolving an initial contour  $C_0(p) = C(p,0)$ . where  $t$  parameterizes the family and  $p$  parameterizes the given contour. The basic result from the front evolution theory is that the geometric shape of the contour is determined by the normal component of the evolution velocity, while the tangential component affects only the parameterization. Hence, after a possible reparameterization, the evolution equation can be written as:

$$\begin{cases} \frac{\partial C(p,t)}{\partial t} = F(C(p,t))\vec{n}(C(p,t)), \\ C(p,0) = C_0(p), \end{cases} \quad (1)$$

where  $F(C(p,t))$  is a scalar function and  $\vec{n}(C(p,t))$  is the unit normal vector along the contour  $C(p,t)$ .

The level set technique represents the contour  $C(p,t)$  implicitly as the zero level set of a smooth, Lipschitz-continuous scalar function  $\Phi(x,t)$ , also known as level set function, where  $x \in \mathcal{R}^2$  in 2D. The implicit contour at any time  $t$  is given by  $C(\cdot,t) = \{x|\Phi(x,t) = 0\}$ . By differentiating  $\Phi(x,t) = 0$  with respect to  $t$  and substituting (1), the following associated equation of motion for the level set function  $\Phi(x,t)$  can be derived:

$$\begin{cases} \frac{\partial \Phi(x,t)}{\partial t} = F(x,t)|\nabla \Phi(x,t)|, \\ \Phi(C_0(p),0) = C_0(p), \end{cases} \quad (2)$$

This work was supported by the Natural Science Foundation of China under Grants 60274009.

H.Cui is with School of Information Science and Engineering, Northeastern University, Shenyang, 110004,China.cuijunhuashi@sohu.com

J.Wu is with School of Information Science and Engineering, Northeastern University, Shenyang, 110004,China.

L.Gao is with School of Information Science and Engineering, Northeastern University, Shenyang, 110004,China.

where  $\nabla$  is the gradient operator and  $|\nabla\Phi(x,t)|$  denotes the norm of the gradient of  $\Phi$ .

### B. Geodesic Active Contour

Let  $C : [0,1] \rightarrow \mathfrak{R}^2$  be a parametrized planar curve and Let  $I : Z^+ \times Z^+ \rightarrow \mathfrak{R}^+$  be a given image in which we want to detect the objects boundaries. Geodesic active contour, as proposed by Caselles et al in [4], is given by

$$\begin{aligned} E[C(p)] &= \int_0^L g(I)(|\nabla I(C(s))|)ds \\ &= \int_0^1 g(I)(|\nabla I(C(p))|) \left| \frac{\partial C}{\partial p}(p) \right| dp \end{aligned} \quad (3)$$

Where  $g$  is a monotonically decreasing function:

$g : [0, +\infty] \rightarrow \mathfrak{R}^+, g(0) = 1, g(x) \rightarrow 0$  as  $x \rightarrow +\infty$ .  $ds$  is the Euclidean arc-length element and  $L$  the Euclidean length of  $C(p)$ . In this paper  $g$  is given as following:

$$g(I) = \frac{1}{1 + |\nabla \hat{I}|^p} \quad (4)$$

where  $\hat{I}$  is an enhanced version of  $I$  and  $p = 2$ .  $\hat{I}$  is obtained through anisotropic selective inverse diffusion proposed by Gilboa et al in [8].

In order to minimize (3), Caselles et al proposed the following geodesic flow:

$$C_t = gk\vec{n} - (\nabla g \cdot \vec{n})\vec{n} \quad (5)$$

Where  $t$  denotes the time as the contour evolves,  $\vec{n}$  is the unit inward normal and  $k$  is the Euclidean curvature.

### C. Gradient Vector Flow Geodesic Active Contour

In [6] Xu and Prince proposed gradient vector flow external force field, known as GVF, which is defined to be the vector field

$$v(x,y) = [u(x,y), v(x,y)] \quad (6)$$

It has large capture range and minimizes the energy function:

$$Q = \int \int \mu(u_x^2 + u_y^2 + v_x^2 + v_y^2) + |\nabla f|^2 |v - \nabla f|^2 dx dy \quad (7)$$

where  $f$  is edge map of enhanced image  $\hat{I}$  and  $\mu$  is weighting parameter. GVF is a dynamic force field, which diffuses along the directions of  $x$  and  $y$  of image gradient simultaneously, and could preserve the image's edge information well after numerous iterations.

Through integrating the normalized GVF (NGVF) into geodesic flow, a new geometric flow for boundary extraction was proposed in [8], given by

$$C_t = \beta gk\vec{n} + (1 - \beta)g(\hat{v} \cdot \vec{n})\vec{n} \quad (8)$$

Where  $\beta$  is a constant parameter that balances the contribution between regularity force and boundary attraction force.  $g$  is defined in (4).  $\hat{v}$  is the NGVF and  $\vec{n}$  is unit inner normal vector.

The balloon force can be integrated to the proposed flow and be used to promote the evolution of active contour when

the NGVF is close to orthogonal to the inward normal. The adaptive balloon force is defined as following:

$$F_{balloon} = \frac{l}{2} e^{-l|\hat{v} \cdot \vec{n}|} \text{sign}(\hat{v} \cdot \vec{n}) \quad (9)$$

where  $l$  is a scale factor and  $l \in \mathfrak{R}^+$ .

The new geometric flow integrated with NGVF and adaptive balloon force is given by:

$$\begin{aligned} C_t &= \beta gk\vec{n} + (1 - \beta)g \left( \left(1 - \frac{l}{2} e^{-l|\hat{v} \cdot \vec{n}|} \text{sign}(\hat{v} \cdot \vec{n})\right) (\hat{v} \cdot \vec{n}) \right. \\ &\quad \left. + \frac{l}{2} e^{-l|\hat{v} \cdot \vec{n}|} \text{sign}(\hat{v} \cdot \vec{n}) \right) \vec{n} \end{aligned} \quad (10)$$

The above boundary-driven geometric flow can handle a larger set of initial conditions compared to the geodesic active contour and improves its segmentation effects.

## III. GEODESIC ACTIVE CONTOUR MODEL INTEGRATED WITH INERTIA

Inertia, a new force field for geodesic active contour, is quite different from traditional force fields. Inertia has the traits of internal force field and external force field. On one hand, it comes from curves themselves represented with the zero level set and is in direct ratio to their evolution velocities at the previous time step. On the other hand, its influence on the evolving curves is constrained by the friction computed from NGVF and the unit normal vector along the contour.

### A. Inertia Force Field

Inertia is used to drive the evolution of geodesic active contours when they get "trapped" by extraneous or undesirable edges due to the invalidation of other external forces.

In a way, that the curves evolve under the action of

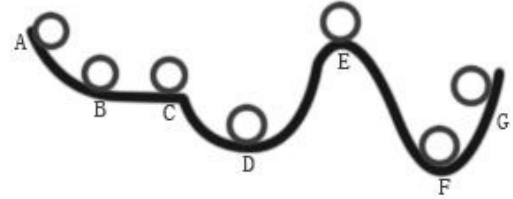


Fig. 1. the function of inertia force

boundary-driven geometric flows defined in (8) and (10) is similar to rolling a ball down a rough slope under the action of gravitation and friction, as is shown in Fig.1. In order to explain the function of inertia force field, We assume that the tangent vector along the slope is equivalent to the normal direction of the point on the evolving curves and the gravity is equivalent to NGVF force. We also assume that the friction is equivalent to the absolute value of the inner product of NGVF and unit normal vector along the curve. The function of inertia is explained as follows:

- Let the ball roll down the slope from the point A, as is shown in Fig.1. When the ball is rolling from B to C,

the gravity is close to orthogonal to the tangent vector along the slope and fails to pull the ball from B to C. If there were no inertia, the ball would stop at B which is a stable NGVF force balance point and corresponds to the position without desirable boundary. If there is inertia and the friction isn't too large, the ball will get across C and reach D which is also a stable NGVF force balance point and corresponds to the point on the desirable boundary.

- Let the ball roll down the slope from C and it will get across D which corresponds to a stable NGVF force balance point without desirable edge. When the ball is rolling from D to E, the NGVF force tries to drag the ball back to D. With the help of inertia force, the ball gets across E and reaches F which is also a stable NGVF force balance point and corresponds to the point on the desirable boundary. It seems that the ball may leave F and continue to roll toward G due to inertia. But it is difficult for the evolving curves to get across the real boundary with high gradient magnitude. The reason is that the function value of  $g$  is very small near the real boundary and the inertia is decreased acutely. Even if the evolving curves get across the real boundary a little, they would be dragged back by NGVF force pointing to the real boundary from its both sides. Thus, the evolving curves will stay at the real boundary in the end.
- It seems that it is the necessary condition for the ball to get across E that point C is higher than point E and inertia is sensitive to initial curve. But in fact, it is inertia that may make the geometric active contour to be less sensitive to initial curve. If the ball rolls down from C with certain initial speed, it can get across E even if C is lower than E.

Inertia force field constrained by friction is given as:

$$F_{friction} = \lambda |\hat{v} \cdot \vec{n}| \quad (11)$$

$$F_{inertia} = \frac{C_t'}{1 + F_{friction}} = \frac{C_t'}{1 + \lambda |\hat{v} \cdot \vec{n}|} \quad (12)$$

Where  $\lambda$  is positive attenuation coefficient which is used to adjust the attenuation speed of inertia force.  $C_t'$  is the velocities of the evolving curves at the previous instant.

### B. Geodesic Flow Integrated with Inertia

We integrate inertia and NGVF into geodesic flow and get the following edge-driven geometric flow:

$$C_t = \alpha g k \vec{n} + \beta g \left( \hat{v} \cdot \vec{n} + \frac{C_t'}{1 + \lambda |\hat{v} \cdot \vec{n}|} \right) \vec{n} \quad (13)$$

where  $\alpha$ ,  $\beta$  and  $\lambda$  are positive constant parameters that balance the contribution among regularity force, boundary attraction force and inertia force.

We can also integrate NGVF, adaptive balloon force and inertia into geodesic flow and get the following edge-driven

geometric flow:

$$C_t = \alpha g k \vec{n} + \beta g \left( \left( 1 - \frac{l}{2} e^{-l |\hat{v} \cdot \vec{n}|} \text{sign}(\hat{v} \cdot \vec{n}) \right) (\hat{v} \cdot \vec{n}) + \frac{l}{2} e^{-l |\hat{v} \cdot \vec{n}|} \text{sign}(\hat{v} \cdot \vec{n}) \right) + \frac{C_t'}{1 + \lambda |\hat{v} \cdot \vec{n}|} \vec{n} \quad (14)$$

The interpretation of above geometric flows is as follows:

- When the contour curves are marching or counter-marching toward object boundary, the NGVF and the inward normal vector have nearly the same or opposite directions ( $|\hat{v} \cdot \vec{n}| \rightarrow 1$ ), the friction is large and the inertia is attenuated maximally. when the NGVF is close to orthogonal to the normal ( $|\hat{v} \cdot \vec{n}| \rightarrow 0$ ), the inertia force is little attenuated and the evolving curves have a tendency to keep original movement state. In this way, geodesic active contour integrated with inertia force and NGVF has the ability to enter into long, thin indentation.
- The function value of  $g$  round the real boundary is very small. When the curves approach the real boundary, their evolving velocities are decreased acutely and the inertia force has very small amount. Thus inertia contributes little to the evolution of the curves. Here geodesic active contour integrated with NGVF and inertia has similar convergence quality with gradient vector flow geodesic active contour .
- The force fields are defined for all level sets, not just the zero level set corresponding to the interface contour curve. But only the forces on the grid points around the zero level set are computed from (13) (or (14)) and the forces on all other grid points are computed through constructing 'extension velocities'.

The evolution of the proposed flows is equivalent to searching for a steady-state solution of the following equations:

$$\begin{aligned} \Phi_t &= F |\nabla \phi| \\ &= \alpha g k |\nabla \Phi| - \beta g \left( \hat{v} \cdot \nabla \Phi + \frac{\Delta \Phi' \cdot |\nabla \Phi|}{1 + \lambda |\hat{v} \cdot \frac{\nabla \Phi}{|\nabla \Phi|}} \right) \end{aligned} \quad (15)$$

$$\begin{aligned} \Phi_t &= F |\nabla \phi| \\ &= \alpha g k |\nabla \Phi| - \beta g \left( \left( 1 - \gamma \left( \hat{v} \cdot \frac{\nabla \Phi}{|\nabla \Phi|} \right) \right) (\hat{v} \cdot \nabla \Phi) \right. \\ &\quad \left. + \gamma \left( \hat{v} \cdot \frac{\nabla \Phi}{|\nabla \Phi|} \right) \text{sign} \left( \hat{v} \cdot \frac{\nabla \Phi}{|\nabla \Phi|} \right) |\nabla \Phi| + \frac{\Delta \Phi' \cdot |\nabla \Phi|}{1 + \lambda |\hat{v} \cdot \frac{\nabla \Phi}{|\nabla \Phi|}} \right) \end{aligned} \quad (16)$$

Due to integrating NGVF and inertia force into geodesic flow, new boundary-driven geometric flows enable active contour to enter into long, thin indentation of the objects' edge and further improve the segmentation effect of geodesic active contour.

### C. Numerical Implementation

Denote a grid point by  $X_i$  and the discrete time scale by  $t_m$ , where  $i, m$  are integers. The resulting level set update equation can be written as

$$\Phi(X_i, t_{m+1}) = \Phi(X_i, t_m) + \Delta t \Delta \Phi(X_i, t_m) \quad (17)$$

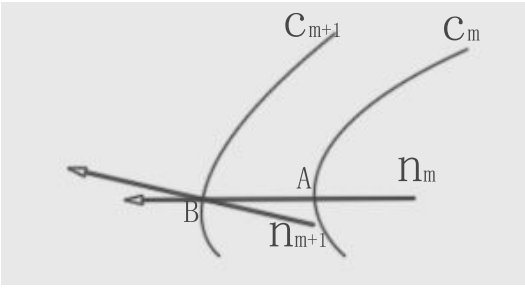


Fig. 2. the transfer of inertia force

Where  $\Delta t = t_{m+1} - t_m$  is the time-step size. Given an initial level set function  $\Phi(\cdot, t_0)$ , (17) can be used to update the level set function at successive time instants  $t_{m+1}$ ,  $m=0,1,\dots$ , until convergence. Although not explicitly computed until the end, the zero level set represents the evolving contour(s).

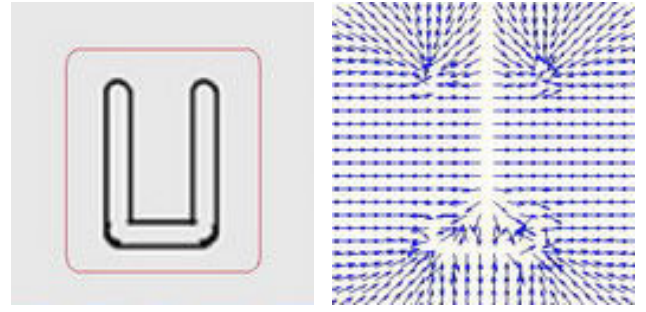
The forces are really only meaningful at the zero level set of  $\Phi$ . Yet, the update equation (17) applies to all values of  $\Phi$ , not just those around zero. In order to extend the force field to all level sets and enable the evolving contours to inherit their velocities at the previous time-step, 'extension velocities' proposed by Sethian and Adalsteinsson in [13] was used in this paper. To initialize the process, the grid points closest to the moving contour inherit the velocities of the closest evolving contour points. Solve the PDE

$$F_\tau + \text{sign}(\phi) \frac{\nabla \Phi}{|\nabla \Phi|} \nabla F = 0 \quad (18)$$

with initial condition  $F=0$  except at these points.  $F$  is a scalar function and specified in (15) and (16). Note that on the contour represented with the zero level set, the force  $F$  does not change, thus preserving the boundary condition. For the implementation, this translates into conservation of the values of  $F$  at these nearby grid points. At convergence, when  $F_\tau = 0$  the solution satisfies  $\nabla \Phi \cdot \nabla F = 0$  which means that  $F$  is a constant along the normals to the level sets. Every level set then evolves with the same speed. Therefore, the velocities of the evolving curves are extended to all level sets. This means that all grid points in the same normal direction inherit the velocity of corresponding grid point closest to the zero level set at the previous time step. After the level set function  $\Phi$  is updated, the grid point, which will become one of the grid points closest to the zero level set at the current time step, can inherit its velocity at the previous time step.

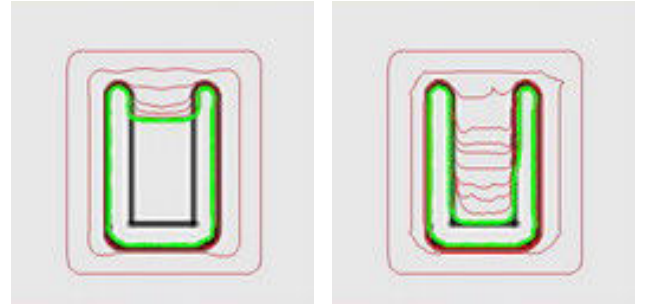
Fig.2 illustrates the transfer of inertia force.  $C_m$  denotes the evolving curve at  $t_m$ .  $A$  is one of the points on the contour curve  $C_m$ .  $n_m$  is the normal at point  $A$  on the curve  $C_m$ .  $B$  is a point of intersection lying on the contour curve  $C_{m+1}$  and the normal  $n_m$ .  $n_{m+1}$  is the normal at point  $B$  on the curve  $C_{m+1}$ .  $(p, q)$  is the coordination of grid point  $B$ .  $F(X_A, t_m)$  is the composition of forces acting on the grid point  $X_A$  at  $t_m$  and is specified in (15) and (16). Inertia acting on the grid point  $X_B$  at  $t_{m+1}$  is given as following:

$$\begin{aligned} \Delta \Phi'(X_B, t_{m+1}) &= F(X_A, t_m) |\nabla \phi(X_A, t_m)| \\ &= F(X_B, t_m) |\nabla \phi(X_A, t_m)| \end{aligned} \quad (19)$$



(a) input image and initial curve

(b) NGVF



(c) geodesic active contour integrated with NGVF

(d) geodesic active contour integrated with NGVF and inertia force

Fig. 3. U shape

$$F_{inertia}(X_B, t_{m+1}) = \frac{\Delta \Phi'(X_B, t_{m+1})}{1 + \lambda |\mathbf{v}(p, q) \cdot \frac{\nabla \Phi(X_B, t_{m+1})}{|\nabla \Phi(X_B, t_{m+1})|}|} \quad (20)$$

The transfer of inertia force is implemented when the component of  $F(X_A, t_m)$  in the direction of the normal  $n_m$  is transferred to  $B$ . The direction of the component of  $F(X_A, t_m)$  is changed from the direction of  $n_m$  to the direction of  $n_{m+1}$ . The magnitude of the component of  $F(X_A, t_m)$  is attenuated by the friction.

#### IV. EXPERIMENTAL RESULT

In this section, we present several experiments which apply the geometric flows integrated with inertia force field. Two synthetic images and two real images have been used for the validation of the proposed inertia force field. Promising experimental results were obtained. In the following figures, the red thin curves denote the initial contour curves and the evolving curves. The green thick curves denote the convergence curve.

We test Fig.3(a) with  $128 \times 128$  pixel. The Fig.3(b) shows the NGVF force field. In the long, thin concavity, NGVF force is nearly opposite, which implies that it can not completely enter into the concavity. The Fig.3(c) shows that geodesic active contour integrated with NGVF fails to completely enter into the concavity. Inertia offers a force pointing to the bottom of the concavity. In Fig.3(d) the initial curve begins to evolve with zero initial speed. It is clearly shown that geodesic active contour integrated with NGVF and inertia force completely enters into the concavity .

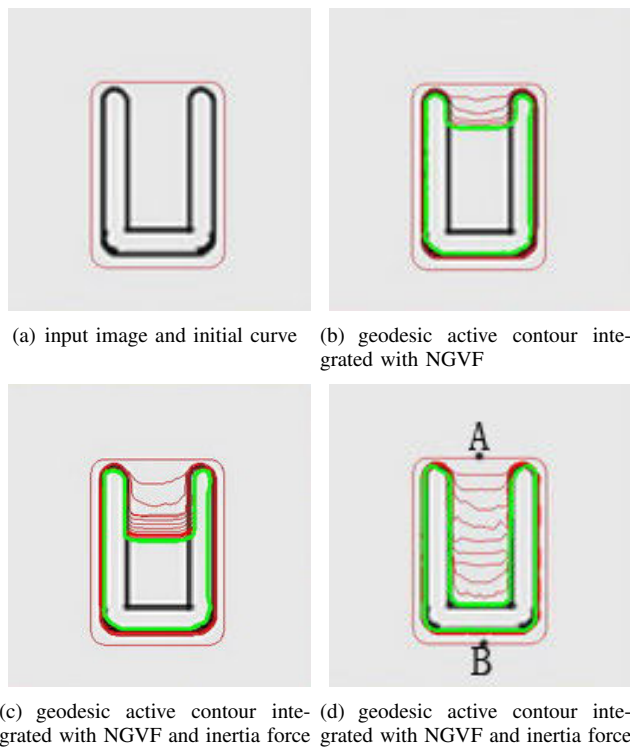


Fig. 4. U shape

In Fig.4 the curve begins to evolve from the new initial position. The Fig.4(b) shows the convergence process of geodesic active contour integrated with NGVF. It is obvious that the curve converge the same position as is shown in Fig.3(c). The influence of initial curve on the evolution of contour curves is shown in Fig.4(c). Though inertia force and NGVF were integrated into geodesic active contour, the evolving curve still fails to enter into the concavity. In order that the curve can completely enter into the concavity, initial speed is given to initial curve. In Fig.4(d) the initial speed of A is equal to 10 in the direction of inner normal and the initial speed of B is equal to 0. The initial speed of the other points on the initial curve is linearly interpolated between A and B. Let the curve begin to evolve with initial speed computed by above-mentioned method. It is clearly shown that the curve completely enters into the concavity.

Fig.5(a) is a medical CT image with  $256 \times 256$  pixel. We test it to illustrate the difference segmentation performance between the geodesic active contour integrated with NGVF and the geodesic active contour integrated with NGVF and inertia force. In Fig.5(d) the initial contour curve begins to evolve with zero initial speed and extracts the boundary successfully. In the above three experiments, the parameters are set as follows:  $\alpha = 0.02$ ,  $\beta = 1$ ,  $\lambda = 0.15$ .

Fig.6 shows a sheet metal gauge with many blob-like concave regions. The original  $240 \times 240$  pixels image and the initial curve are shown in Fig.6(a). The Fig.6(b) shows the NGVF force field. The Fig.6(c) shows that geodesic active contour integrated with NGVF and adaptive balloon force cannot extract any blob-like concave. In Fig.6(d) geodesic

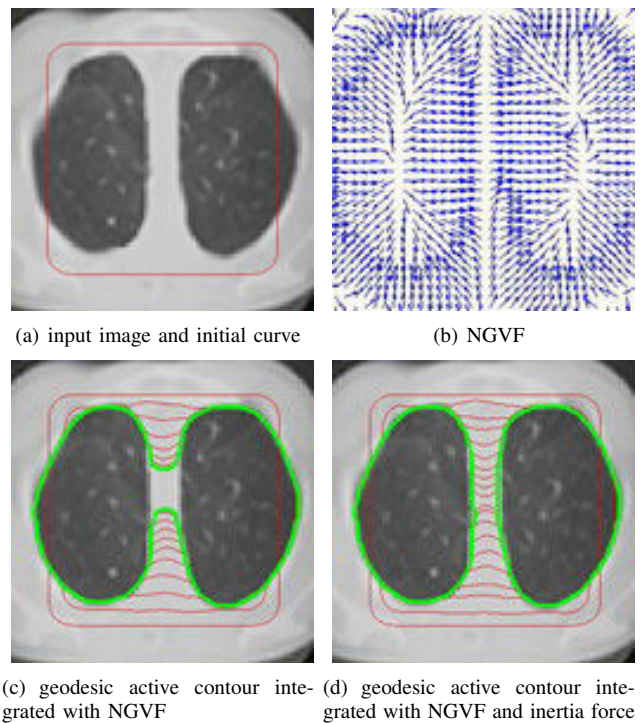


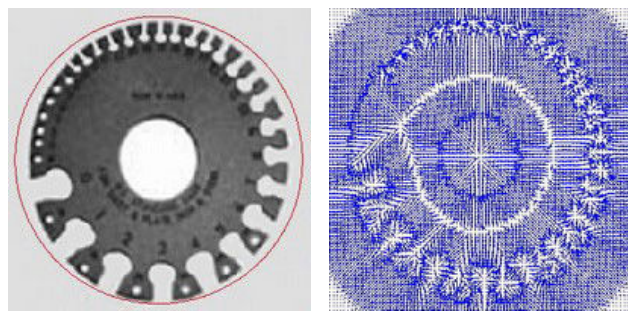
Fig. 5. Medical CT image

active contour integrated with NGVF, adaptive balloon force and inertia force begins to evolve with initial speed which is equal to 10 in the direction of inner normal on every initial contour point. The geodesic active contour integrated with NGVF, adaptive balloon force and inertia force overcomes the resistance coming from NGVF when it tries to enter into blob-like concaves. It is clearly shown that it extracts most of them successfully in different directions around the circular disc, except for those gaps which have increasingly high curvature of those structures. In this experiment, the parameters are set as following:  $l = 1$ ,  $\alpha = 0.02$ ,  $\beta = 1$ ,  $\lambda = 0.1$ .

Fig.7(a) and Fig.7(c) shows two hexagram images blurred by 20% and 30% impulse noise respectively. On one hand, that inertia is integrated to geodesic active contour increases the probability that active contour leaks through the weak edge; On the other hand, inertia is constructed on the base of NGVF force field so that its anti-jamming ability highly depends on the quality of edge map which is used to calculate NGVF. In order to avoid weak-edge leakage, we use anisotropic selective inverse diffusion to enhance edge in the presence of noise. It is shown in Fig.7(b) and Fig.7(d) that despite that noise blurs the edge, geodesic active contour integrated with NGVF, adaptive balloon force and inertia force does not leak through the blurred boundary and converges the real boundary successfully.

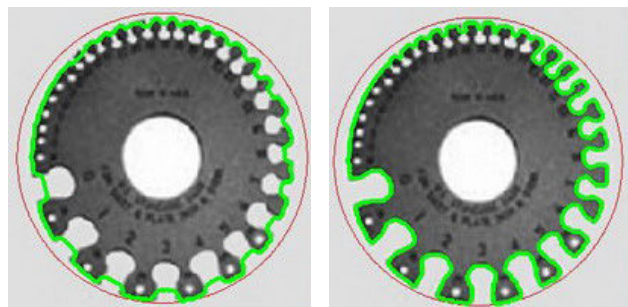
## V. CONCLUSIONS AND FUTURE WORKS

We have introduced a new force field for geometric active contours, which is called the inertia force field. The inertia force field is in direct ratio to evolution velocities of contour



(a) input image and initial curve

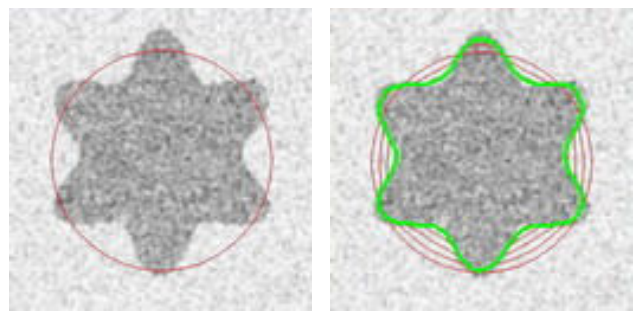
(b) NGVF



(c) geodesic active contour integrated with NGVF and adaptive balloon force

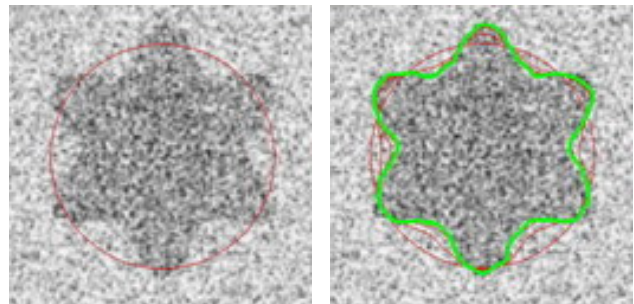
(d) geodesic active contour integrated with NGVF, adaptive balloon force and inertia force

Fig. 6. Metal gauge



(a) input image and initial curve

(b) geodesic active contour integrated with NGVF, adaptive balloon force and inertia force



(c) input image and initial curve

(d) geodesic active contour integrated with NGVF, adaptive balloon force and inertia force

Fig. 7. Noisy hexagram image

curves at the previous time step. Its effect on the evolving contour curves is constrained by the friction computed from image data and contour curves. We integrated both inertia force field and other force fields into geodesic active contour and gained new geometric flows for boundary extraction. Experimental results show that the new geometric flows enable contour curves to enter into into long, thin indentation.

Further investigations into the character and use of inertia force field are warranted. In particular, constructing the inertia force in other force fields may be helpful to the application of inertia force.

#### REFERENCES

[1] M. Kass, A. Witkin, and D. Terzopoulos, Snakes: Active contour models, *International Journal of Compute Vision*, vol. 1, pp. 321-331, 1987.

[2] V. Caselles, F. Catte, T. Coll, and F. Dibos, A geometric model for active contours, *Numer. Math.*, vol. 66, pp. 1-31, 1993.

[3] V. Caselles, R. Kimmel, and G. Sapiro, Geodesic Active Contours, *International Journal of Computer Vision*, vol. 22, pp. 61-79, 1997.

[4] Malladi, R., Sethian, J.A., Vermuri, B.C., 1995. Shape modeling with front propagation: A level set approach. *IEEE Transactions on Pattern Analysis and Machine Intelligence*. 1995, 17 (2), 158-175.

[5] Cohen, T.F, On active contour models and balloons, *Image Understanding*, 1991, 53(2), 211-218.

[6] Xu Chen-Yang, Jerry.L. Prince. Snakes, Shapes, and Gradient Vector Flow. *IEEE Transactions On Image Processing*, March 1998, Vol. 7, No 3.

[7] F.T. Chan, L. Vese, Active contours without edges, *IEEE Transactions On Image Processing*, 2 (2001) 266-327.

[8] G. Gilboa, Y. Zeevi, N. Sochen, Anisotropic selective inverse diffusion for signal enhancement in the presence of noise, *Proc. IEEE ICASSP-2000*, vol. I, pp. 211 -224, June 2000.

[9] Paragios N, Mellina-Gotardo o, Ramesh V. Gradient vector flow fast geodesic active contours. *IEEE Transactions on Pattern Analysis and Machine Intelligence*. 2004, 26(3), 402-407.

[10] S. Osher and J.A. Sethian, *Fronts Propagating with Curvature-Dependent Speed: Algorithms Based on Hamilton-Jacobi Formulations*, *J. Computational Physics*, vol. 79, pp. 12-49, 1988.

[11] J.A. Sethian, *Level Set Methods and Fast Marching Methods*. Cambridge, UK: Cambridge Univ. Press, second ed., 1999.

[12] J.A. Sethian, A Fast Marching Level Set Method for Monotonically Advancing Fronts, *Proc. Natl Academy of Sciences*, vol. 93, pp. 1591-1595, 1996.

[13] Adalsteinsson, D. and Sethian, J. A. The fast construction of extension velocities in level set methods. *J. Comp. Phys*, 1999, 148:2-22.

[14] Adalsteinsson, D. and Sethian, J. A. A Fast Level Set Method for Propagating interfaces. *J.comp.phys*.1995,118-2,pp 269-277.